

Applications of particle tracking microscopy methods on biomaterials research

A. Papagiannopoulos

Theoretical and Physical Chemistry Institute, National Hellenic Research Foundation, 48 Vassileos Constantinou Avenue, 11635 Athens, Greece

The key concepts and theoretical background of particle tracking methods are presented based on their fundamental applications on the microrheological characterization of complex fluids. The versatility and efficiency of particle tracking methodology is demonstrated by its use in a wide range of materials i.e. hydrogels, tissues, complex systems from food science, biological fluids and mechanical response of cells. The ability of particle tracking microscopy to probe local structure and rheology makes it a technique that complements bulk rheology and expands our understanding in multi-length scale soft materials, a class that includes biomaterials.

Keywords: particle tracking; microrheology; hydrogels; biopolymers; polysaccharides; cells

1. Introduction

The development of microrheological techniques in the previous decade gave access to rheological properties of soft materials with spatial sensitivity at the micro and nano scales[1]. In particular, tracking of tracer particles within complex matrices provided measurements with great versatility such as the remarkable mapping of the mechanical properties inside live cells[2]. During the last decade the researchers develop and use particle tracking methodologies to investigate a great variety of systems. Diffusion of nanoparticles has been investigated to characterize the trapping ability of human respiratory mucus[3], mechanics of cells and extracellular matrix were correlated with the grade and stage of tumors[4] while permeation of drug-loaded polysaccharide nanoparticles through transdermal routes have been monitored[5]. Additionally, fusion of the HIV-1 viral and plasma membrane and release into the cytoplasm has been supported by single particle tracking of labeled viral particles[6]. The micromechanical characteristics and porosity of hyaluronic acid-based hydrogels have been accessed by multiple particle tracking microrheology[7] and the mechanical stresses generated by single cells has been probed by fluorescent beads trapped in the surrounding elastic network [8]. Nanoparticle tracking has been used for sizing[9] and multiple particle tracking for probing viscoelasticity[10] in food hydrocolloids. These are representative examples that are included in this chapter in order to highlight the interesting recent advances in particle tracking techniques and point the possibilities for the near future.

2. Particle tracking for microrheological investigations

Microrheology methods provide information on mechanical properties at a local level. With passive microrheology, which is mainly described here, the thermal motion of probe particles inside biomaterials is monitored. In active microrheology probe particles are forced to move by external forces. Microrheology has the advantages of very small sample amounts, local measurements and extended time (or frequency) range. Random thermal motion of a micro-sized particle is defined by the mechanical properties of the fluid. The mean-squared-displacement (MSD) of thermally fluctuating probe particles as a function of time (lag time τ) contains information on the viscoelasticity of the surrounding fluid[11].

Thermal Brownian fluctuations are described by a random walk. the MSD of the particle is provided by equation 1.

$$\langle \Delta r^2(\tau) \rangle = \langle (\vec{r}(t + \tau) - \vec{r}(t))^2 \rangle_{t,N} \quad (1)$$

where $\vec{r}(t)$ is the particle trajectory and the average is over all initial times (t) and over all particles in the ensemble (N). In simple Newtonian fluids MSD is proportional to lag time (equation 2).

$$\langle \Delta r^2(t) \rangle = 6Dt \quad (2)$$

The diffusion coefficient D is connected to the fluid viscosity by Stokes-Einstein equation $D = \frac{k_B T}{6\pi\eta a}$. When particle radius a is known then one can define viscosity η or inversely when fluid viscosity is known independently then one can define the hydrodynamic size of the particle.

In complex fluids (non-Newtonian) the contributions from viscous and elastic properties (quantified by the storage and loss moduli, G' and G'') make the MSD time-dependence non-trivial. In a purely viscous material $\langle \Delta r^2(\tau) \rangle \sim \tau$ while

in a purely elastic material $\langle \Delta r^2(t) \rangle \sim k_B T$ as the particle is restricted by the elastic medium. In a viscoelastic fluid MSD scales as $\langle \Delta r^2(\tau) \rangle \sim \tau^\beta$ with $0 < \beta < 1$ and the scaling exponent β is generally time-dependent. The viscoelastic modulus is connected to the MSD by the generalized Stokes-Einstein equation[11] which in Fourier space is written as in equation 3 with $\langle \Delta r^2(\omega) \rangle$ the Fourier transform of the MSD.

$$G^*(s) = \frac{k_B T}{\pi i \omega a \langle \Delta r^2(\omega) \rangle} \quad (3)$$

Video particle tracking (VPT) is a widely used method to extract the MSDs from embedded colloidal particles inside biomaterials. It has the capability of separately tracking individual particles and therefore allows for local mapping. An optical microscope connected to a CCD camera is an effective realization of the method. Spherical colloidal microparticles (~250-500 nm in radius) are immersed into the fluid in a concentration such that 50-100 particles are in focus at the same time. The motion of the particles is recorded by a DVD recorder, an integrated frame grabber or a video capturing software. The acquisition rate is normally in the order of 25-30 frames per second. More technical details can be found in a dedicated book chapter[12].

Image analysis software (IDL, MATLAB etc) is used to extract the trajectories of particles with the aid of particle tracking algorithms which locate the positions of the particles in each frame and produce their trajectories. Basic details on particle tracking procedures can be found in J. Crocker and D. Grier[13]. In brief, every frame of the complete movie is a 2-D array that contains the brightness of the corresponding pixels on the plane of view. Local maxima in brightness are picked as possible probe particles and their position is estimated as the centroid of every bright object. Particles may be distinguished from other features in the image by applying filters based on their shape (roundness), size and total brightness. The 2-D trajectory $\vec{r}(t)$ of every separate particle is extracted and the MSD of every particle or the ensemble average MSD is calculated (equation 1). In addition histograms of displacements and particle MSD distributions may be obtained.

Microrheological measurements are local by nature and a micro or nanoparticle experiences its local surroundings via its surface. Therefore a microrheological measurement reflects the bulk properties of the fluid only if (1) the fluid's inhomogeneities are at length scales smaller than the particle size (e.g. the correlation length in a semi-dilute polymer solution or the mesh size in a gel network is smaller than the particle's size) and (2) the interactions between the particle and the fluid components are neither attractive (sticky particle) or repulsive (depletion layer). Of course measurements that are affected by the local environment are valuable for accessing local properties and quantifying heterogeneities. Average bulk properties can be estimated by extracting the correlations between distant particles within the fluid[12] (two-point correlation).

3. Hydrogels and tissues

Hydrogels are swollen polymeric networks whose volume is mainly filled by aqueous media. In biomaterials, biopolymers are very often used as building units of hydrogels. Networks are formed by cross-links that maybe chemical or physical. A bottom-up approach was presented for the immobilization of bioactive factors on collagen variants. Cysteines were introduced to native collagen in order to strengthen its mechanical capabilities while preserving its triple-helical structure. The added groups were precisely placed along the biopolymer backbone by the aid of full length collagen-mimetic proteins and acted as cross-linking sites to promote myofibroblast differentiation. PEGylated amine-functionalized polystyrene fluorescent particles were utilized for particle tracking microrheology experiments on the formation of the hydrogel.

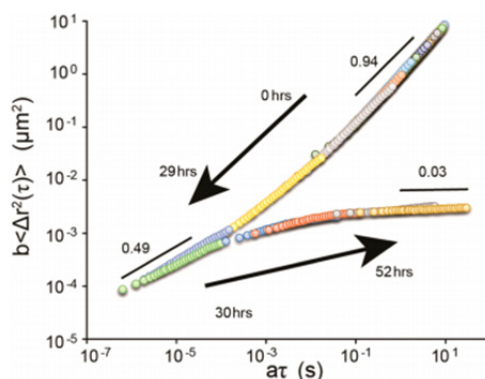


Fig. 1 Pregel and postgel master curves in collagen/cysteine hydrogels. Reprinted with permission from [14]. Copyright 2014 American Chemical Society.

Hydrogel formation in collagen variants has been represented by master curves (Fig. 1) as in the work of Larsen and Furst [15]. In the pre-gel state the subdiffusive regime $MSD \sim \tau^\beta$ with $\beta \approx 1/2$ in Fig. 1 terminates with viscous behaviour at long times. In the post-gel stage particles MSD has an asymptotic behaviour caused by the elasticity of the network. The MSD vs τ curves are grouped in two master curves i.e. pre-gel and post-gel master curve. The normalization parameters (b for MSD and α for τ) are customarily plotted as a function of reaction time and this way the gelation process is characterized in terms of critical phenomena[14]. This method of time-cure superposition has been also applied on the kinetics of gelation of collagen-inspired biopolymers expressed by transgenic yeast *P. Pastoris*. Upon cooling the collagen-like end blocks create well-defined transient nodes at the ends of random coil hydrophilic blocks. This work presents the efficiency of passive multiple particle tracking microrheology in the characterization of hydrogel formation[16].

Upconversion nanoparticles emit visible light by excitation in the near infrared. It has been shown that the fluorescence intensity of NaYF₄:Yb nanoparticles (30 nm in size) were synthesized and coated by poly(allylamine hydrochloride) in order to displace the hydrophobic ligands on their surface. They were subsequently incorporated into gelatin methacryloyl hydrogels by addition before initiating the cross-linking reaction. The decrease in fluorescence intensity was in good agreement with the one of fluorescein isothiocyanate that was conjugated with the hydrogels in a 7-day period of degradation in daily-refreshed PBS solution. Degradation of the hydrogels was also monitored by their change in weight. Interesting results were obtained with *in vivo* studies in rat abdomens. The signals from upconversion nanoparticles were capable of probing the hydrogel degradation within the tissue while the fluorescein isothiocyanate fluorescence was not detectable through the tissue. Slicing the tissue in sections and observation under confocal microscope was consistent with the results from the nanoparticles. The proposed system did not imply any possibilities of causing side effects and or inflammation and edema[17].

Tissue engineering for the generation of cartilage is based on the introduction of chondrocytes in three-dimensional scaffolds that are normally hydrogels i.e. 3-D polymeric networks with highly hydrophilic nature that are able to withstand mechanical loads and create a porous aqueous environment. Their local environment plays an important part in the preservation of chondrocyte phenotypes i.e. spherical morphology and high expression of collagen II and glycosaminoglycans. The “edge-flourish” phenomenon utilizes the presence of microspherical cavities and multiple edges to promote the accommodation and outgrowth of cells provides higher proliferation and extracellular matrix secretions sustainability. The mechanical characteristics of this biological phenomenon have been studied by methods based on particle image velocimetry and multiple particle tracking. Chondrocytes from porcine articular cartilage were encapsulated in agarose hydrogels and the surface stresses were explored by finite element analysis. Probing the displacements of fluorescent microbeads at the edges and in the bulk by fluorescent microscopy the authors managed to quantify the enhanced outward surface tensions generated by the outgrowth of the cells. They highlighted the importance of the edge-flourish layer and the potential of their study as a platform for further developments in this direction[18].

The mechanical properties of the extracellular matrix are defined not only by its constituents but also by the incorporated cells. At the same time the mechanical stresses of the matrix that are exerted on the cells regulates crucial cell processes. Methods that probe the bulk mechanical properties of the extracellular matrix are not sensitive to the dynamics in the proximity of the cell and therefore techniques with relevant spatial and temporal sensitivity are needed. Carboxylated microbeads were embedded in collagen gels in order to study the biomechanical environment of dermal fibroblasts and human aortic smooth muscle cells. The microbeads were controlled by optical tweezers in order to map the material response in the pericellular region. Elastic and plastic deformation was observed and it was reported that elasticity spanned three orders of magnitude near a single cell, much higher than in cell-free matrices. Stiffness heterogeneity could be softened by inhibition of cell contractility. It was suggested that biomaterial scaffolds design should take the inhomogeneous pericellular stiffness into account[19].

Hyaluronic acid-based cryogel scaffolds were investigated by multiple particle tracking microrheology. Elasticity of the polymeric matrix was characterized locally by observing the MSDs of individual probe particles while the non-Gaussian parameter indicated a fairly inhomogeneous medium. Additionally particles tracked within the pores revealed that the fluids (water or water/glycerol mixtures) was homogeneously distributed inside without signs of dissolved uncrosslinked hyaluronic acid chains. The plateau modulus from microrheology was calculated from the plateau of the 2-D MSD as $G_0 = \frac{2k_B T}{3\pi a MSD}$ (where a the particle radius) to be about 10 Pa. This value was two orders of magnitude lower than the one obtained by traditional bulk rheology. Possible explanations for this discrepancy were the contribution of stretched chain segments in the bulk rheometry experiment and the presence of highly cross-linked regions where the probe particles could not enter. In any case the authors marked that the local modulus, measured by particle tracking, is the most relevant to cell culture. This work was reported as the first one to characterize elastic and viscous behavior in porous hydrogels by the employment of multiple particle tracking microrheology[7].

4. Drug delivery, diffusion and sizing

Sizing of nanoparticles in biological media is very crucial for biomedical imaging and nanodelivery applications. Fluorescent single particle tracking has been applied successfully on monitoring the aggregation of drug nanocarriers in undiluted whole blood. Based on the maximum entropy analysis valuable insights to the aggregation were feasible. The proposed tool was considered promising for pharmacy and related fields[20].

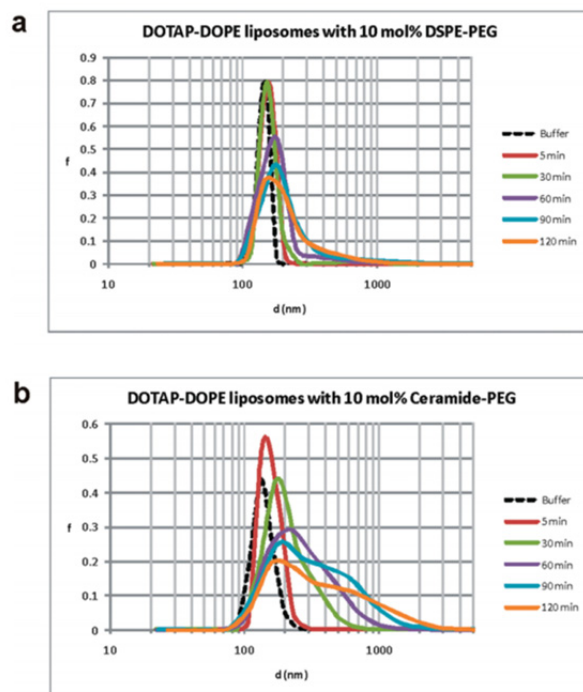


Fig. 2 Effect of liposome PEGylation on size e.g. 10 mol % DSPE-PEG (a) and ceramide-PEG (b). Reprinted with permission from [20]. Copyright 2010 American Chemical Society.

In Figure 2 the evolution of size of liposomes in different PEG agents is presented. With 10 mol % DSPE-PEG (Fig. 2a) liposomes are stable while at ceramide-PEG 10 mol % (Fig. 2b) size increases over time and additionally a second larger population appears. The compromise in stability is caused by the diffusion of ceramide-PEG lipids out of the liposome membranes in the blood[20].

Delivery of siRNA *in vitro* has been developed by dextran nanogel carriers. The size distributions of the nanocarriers in HEPES buffer and citrated human plasma at 37 °C were obtained by single particle tracking and were evaluated for intravenous delivery by single particle tracking. It was found that PEGylation was necessary to prevent particle aggregation. In blood, aggregation not only compromises biodistribution but also causes toxicity[21]. Nanogels of ornithine methacrylamide have been cross-linked by carbon dots which provided stable fluorescence signals. This way the controlled release of dextran was explored. In addition, cellular uptake and internalization without and with conjugation with folic acid were tested[22].

Permeation experiments on mice skin that were carried out *ex vivo*, showed great potential for applications in transdermal drug delivery. Chitosan nanoparticles loaded with curcumin were tracked by confocal laser scanning microscopy imaging (FITC-labeled chitosan). Skin pieces were loaded with the nanoparticles in Franz diffusion cells for 8 hours. The pathways of penetration were afterwards scanned at various depths by optical sectioning in skin layers. It was observed that penetration was deeper when it was through hair follicles. This was a straight conformation that hair follicles is the route for transdermal delivery[5].

5. Biopolymer complex fluids

Particle tracking methods including nanoparticle tracking analysis and microrheology are promising for the investigation of complex fluids[1] as for example in hydrocolloids for the food industry. Modern food science includes the study of nanostructured food and nanodelivery of bioactive substances and hence tracking of exogenous or endogenous nanoparticles provides important information on local structure and mechanical properties and diffusional processes[23]. Materials as food gels and emulsions are multicomponent and heterogeneous complex fluids with hierarchical organization. Their mechanical behavior is therefore length-scale dependent and consequently microrheology methods offer the possibility to extend traditional rheology to the micro and nano level[24].

Xanthan solutions were investigated by video particle tracking microrheology (VPTMR) [10]. Its rheological properties were documented as power-law dynamics that revealed the complex self-similar morphology of xanthan fluids. Power-law viscoelasticity $G \sim \omega^\beta$ was naturally revealed by the MSD i.e. $\text{MSD} \sim \tau^\beta$ of 0.5 μm PS nanospheres (Fig. 3, left). The magnitude of the modulus increased while the power-law exponent decreased with xanthan concentration as the viscosity and the relative elasticity increased. Cox-Merz rule was utilized for a direct comparison of the MSD data (linear experiment) to the shear-thinning parameters obtained by viscometry (non-linear experiment).

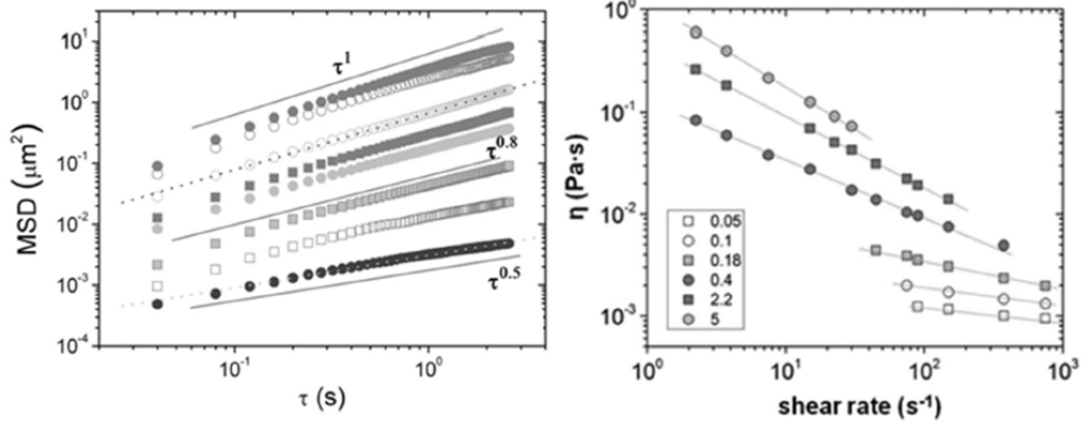


Fig. 3 Left: MSD from particle tracking experiments in xanthan solutions with no added salt at 0, 0.08, 0.18, 0.40, 0.90, 1.4, 2.2 and 3.3 mg/ml (from top to bottom). Lines are representative fits with equation 4. Right: Steady-shear viscosity for xanthan solutions with no added salt (concentration in mg/ml is indicated). Lines are fits with equation 5. Reprinted from [10], Copyright 2016, with permission from Elsevier.

In more detail the power-law behavior of the MSD was modeled by equation 4.

$$\langle \Delta r^2(\tau) \rangle = A \cdot \tau^\beta \quad (4)$$

The Fourier transform of an MSD that is described by a power-law can be written analytically and hence equation 3 leads to a power-law in frequency for the complex modulus [10] (equation 5).

$$|G^*(\omega)| = \frac{k_B T}{\pi a A \cdot \Gamma(\beta + 1)} \cdot \omega^\beta \quad (5)$$

The non-linear viscometry experiment provides the flow curves of xanthan solutions (Fig. 3, right). The shear thinning behavior is modeled by equation 6 which defines the flow index m and a prefactor N .

$$\eta(\dot{\gamma}) = N \cdot \dot{\gamma}^{-m} \quad (6)$$

Complex viscosity is derived by equation 5 as $\eta^*(\omega) = \frac{|G^*(\omega)|}{\omega} = \frac{k_B T}{\pi a A \cdot \Gamma(\beta + 1)} \cdot \omega^{\beta-1}$ and it can be compared with the steady-state viscosity for $\omega = \dot{\gamma}$.

Hence, a low-cost technique (VPTMR) could give information on an industrially relevant property (viscosity). The power of VPTMR to characterize a food complex fluid was further confirmed by testing denaturation/renaturation protocols and salt content/valence in xanthan [10]. Scaling of the viscosity of xanthan as a function of concentration at various conditions was discussed in terms of double-helix induced inter-chain associations and comb polyelectrolyte behavior.

Electrostatic complexation of the anionic polysaccharide xanthan with the cationic surfactant dodecyltrimethylammonium bromide (DTMAB) leads to hydrophobic modification of the otherwise hydrophilic polyelectrolyte. VPTMR was combined with viscometry and light scattering methods. At low ionic strength the binding of the surfactant is more effective than at high salt content. Additionally, complexation in the melted-state of xanthan has more intense results. In general the hydrophobic modification transforms the solutions from soft interconnected networks to independently diffusive aggregates [25]. This work demonstrated how practical applications in food science and soft matter can be designed, based on the knowledge on complex food polysaccharide fluids.

β -Glucans are viscous and gel forming polysaccharides. They have the properties of soluble dietary fibers and may be present in natural foods or in formulated products. The formation of network in β -glucans isolated from cereals was monitored as a function of storage time by bulk rheology, confocal microscopy and particle tracking microrheology. Bulk rheology followed the increase in elastic modulus and the decrease in phase angle as. Confocal microscopy

depicted the formation of clusters that jammed together during aging. Particle tracking microrheology showed that the ensemble averaged MSD of carboxylate-modified fluorescent microspheres (0.75 μm) gradually dropped both in magnitude and power-law exponent naturally revealing the transformation from a viscous fluid to an elastic solid. Additionally the authors examined the non-Gaussian parameter $N_g = \frac{\langle \Delta x^4(\tau) \rangle}{3(\Delta x^2(\tau))^2} - 1$. N_g is zero for a homogeneous system and greater than zero for an inhomogeneous system. The parameter N_g increased significantly near the gelation point which revealed that the microenvironment experienced by the probe-particles is highly porous and characterized by the presence of polysaccharide chain clusters with different sizes. This work successfully combined microscopic and macroscopic techniques and managed to reveal the formation of network in an important polysaccharide with obvious applications in food industry[26].

6. Mucus layer

Mucus is a complex fluid that is secreted in the eye epithelium, urogenital tract and gastrointestinal tract. It protects the organism against foreign particles and pathogens and toxins. Its rheological and mechanical role is to reduce friction between surfaces. Mucus forms gels at acidic pH and this way protects stomach from the gastric acids during digestion. Georgiades et al.[27] studied well characterized porcine gastric and duodenal mucins as models for human mucins. They used particle tracking microrheology to explore their viscoelasticity and analyzed their results on the established background of linear and grafted polyelectrolytes. Experiments were performed with carboxyl modified PS microspheres (505 nm) while PEGylated particles gave similar results. The scaling of viscosity in pig gastric mucin as a function of mucin concentration was what is expected for flexible polyelectrolytes ($\eta \sim c^{1/2}$) while above the critical entanglement concentration very strong dependence was observed ($\eta \sim c^4$). Below the entanglement concentration MSDs are diffusive i.e. $MSD \propto \tau^\beta$ with $\beta \approx 1$ while inside the entangled regime viscoelasticity manifests itself with subdiffusive MSDs i.e. $MSD \propto \tau^\beta$ with $\beta < 1$. The strong concentration dependence of the viscosity in the entangled regime was attributed mainly to the entanglement of both the main and the side chains of mucin. In porcine duodenal mucin viscosity scaled as $\eta \sim c^5$. Both mucins form gels upon a pH drop as exposure of hydrophobic regions and protonation of salt bridges cause mucin chains to self-assemble. Agents as urea dissolve the gels while ECGC cross-links pig gastric mucin[27].

Polyethylene glycol (PEG) has been increasingly used in drug delivery because of its “stealth” properties. Nevertheless investigations have identified possible immune responses after prolonged or repeated therapies with PEGylated formulations. The reduction in efficiency of these drugs was reported to be caused by induced antibodies that bind to PEG. Virus-binding IgG antibody creates low-affinity cross-links with mucins resulting to virus immobilization as for example in vaginal Herpes infection in mice. Lai et al. demonstrated that anti-PEG IgG and IgM prevent the access of PEG-coated nanoparticles to the vaginal epithelium. immobilize by trapping them in the vaginal mucus gel. Fluorescent carboxyl-modified polystyrene nanoparticles (100 nm) were covered by methoxy poly(ethylene glycol) amine via carboxyl-amine reaction. Experiments were performed on mouse cervicovaginal mucus (mCVM)[28]. The diffusive motion for nanoparticles in mCVM treated with different antibodies was demonstrated. Binding of anti-PEG IgG significantly reduces both the magnitude and slope of the MSD in comparison to control IgG. Control IgG does not lead to restriction in particle diffusion which supports that binding of IgG to PEG is specific. Diffusivities (obtained by $MSD = 4D\tau^\beta$) showed the differences between the two cases. Particle displacements were compared to the particle diameter in order to distinguish between two categories. The displacements that were smaller than the particle diameter were considered to correspond to trapped local motion that follows the thermal fluctuations of the gel itself [28].

Respiratory mucus protects the body from inhaling pathogenous microorganisms and particulates by trapping intruding entities. The role of size and surface properties of particles in mobility through respiratory mucus is a field still open for research. Nanoparticles with dense layers of low molecular weight PEG show minimal mucoadhesion. They were used for comparison with uncoated nanoparticles regarding their diffusion through human respiratory mucus from endotracheal tubes from patients with no lung disease. PEG-coated nanoparticles (size 100 and 200 nm) penetrate mucus at rates many times faster than the uncoated particles. The mucus mesh pore-size becomes evident as particles with diameter larger than 500 nm are sterically trapped. The authors analyzed the motion of PS-COOH and PS-PEG nanoparticles in terms of their diffusivity and MSD scaling exponent. It was clearly shown that in PS-COOH nanospheres diffusion was strongly hindered ($a \sim 0.7$) in comparison to PS-PEG ($a \sim 0.9$) for 100 nm diameter. The diffusivity (at $\tau = 1\text{s}$) was more than ten times higher in PS-PEG. For 500 nm diameter the differences were small. This work shows how the design of therapeutic nanoparticles can be evaluated by studies that include particle tracking[3].

PEGylation has been exploited to produce nanoparticles that are able to penetrate the highly viscoelastic mucus in the condition of chronic rhinosinuitis. PEGylated nanoparticles (200 nm) were found able to pass through mucus and hence promising the underlying epithelial cells [29].

7. Particle tracking in cells and extracellular matrix

Cells and tissue dynamics play an important role in cancer initiation, progression and metastasis. Tumor cells and other cell types communicate through the extracellular matrix that defined their microenvironment. Carboxy-modified fluorescent polystyrene particles were monitored by an epifluorescence microscope for particle tracking microrheology experiments. Normal human mammary fibroblasts and cancer associated fibroblasts were cultured in microscaffolds based on porous gelatin microbeads. Microrheological data from the microtissues differentiated between the two types of cells. MSDs in cancer-activated fibroblasts had larger magnitude which showed cytoskeleton with lower degree of assembly. This result was correlated with the stiffness of the extracellular matrix. A higher degree of collagen assembly was observed in the case of normal fibroblasts[30].

Imaging of human immune deficiency virus type-I (HIV-1) in cells in real time offers the opportunity to define the spatial and temporal infection regulation. The virus can be visualized after labeling along with the nuclear import and integration into the host genome and expression of viral protein. Trajectories of single viral complexes reveal the entering into the nucleous after uncoating i.e. loss of capsid protein from the viral core. The path of the capsid protein marker was divided in three parts; cytoplasmic transport, docking and intra-nuclear[31]. HIV-1 cores after fusion which uncoated close to the nucleus underwent restricted motion as revealed by their MSD[32].

Mechanical stresses generated by single cells were investigated in a methacrylated alginate gel. The stresses exerted to the surrounding environment during cell growth may be important for health. The authors quantified the stress distribution in 3-D as they are able to alter the microenvironment in their vicinity. Confocal fluorescence microscopy provided two 2-D images one for cells (green stain) and one for fluorescent beads (red). Treating the cells with a hyperosmotic solution caused their shrinkage and their detachment from the hydrogel. The elastic network subsequently relaxes (within 5-8 min). Gel deformation was evaluated by the displacements of the embedded probe particles (MATLAB) so that the displacement field was determined. Meshes on the initial cell surface were created by COMSOL. The distribution at the interface between the gel and the cell was found inverse to the mean curvature of the surface and the distance from the geometric cell centre. The average interface stress increased with increasing stiffness of the hydrogel. The proposed hydrogel-based microscopy method could be applied to other cell-hydrogel systems for further investigations on the mechanical interactions of cells with their environment[8].

8. Concluding remarks

The use of particle tracking methods to probe local structure and dynamics in biomaterials is a field that finds increasing interest. It utilizes established microscopy techniques and gains from the many different choices in terms of visualization (e.g. brightfield and fluorescent) and particle size and surface chemistries. This way the properties of biomaterial matrices can be explored in different length scales, types of interactions and contrast conditions. Large size particles probe dynamics that are close to average bulk dynamics while small size particles explore the local structure and inhomogeneities in relevant length-scales. Similarly particles that stick to the components of the fluid provide insights to their individual motion while inert nanoparticles explore the whole of the microenvironment. Advances in measuring cell mechanics, extracellular matrix rheology, food hydrocolloids, hydrogel scaffolds for tissue engineering and drug-loaded nanoparticles are only some examples that show the promising future of these methods.

References

- [1] Waigh TA. Microrheology of complex fluids. *Reports on Progress in Physics*. 2005;68(3):685.
- [2] Tseng Y, Kole TP, Wirtz D. Micromechanical mapping of live cells by multiple-particle-tracking microrheology. *Biophysical Journal*. 2002;83(6):3162-76.
- [3] Schuster BS, Suk JS, Woodworth GF, Hanes J. Nanoparticle diffusion in respiratory mucus from humans without lung disease. *Biomaterials*. 2013;34(13):3439-46.
- [4] Panzetta V, Musella I, Rapa I, Volante M, Netti PA, Fusco S. Mechanical phenotyping of cells and extracellular matrix as grade and stage markers of lung tumor tissues. *Acta Biomaterialia*. 2017;57:334-41.
- [5] Abdel-Hafez SM, Hathout RM, Sammour OA. Tracking the transdermal penetration pathways of optimized curcumin-loaded chitosan nanoparticles via confocal laser scanning microscopy. *International Journal of Biological Macromolecules*. 2018;108:753-64.
- [6] Sood C, Marin M, Melikian GB. Characterization of HIV-1 Entry Site Specificity using Single-Particle Tracking. *Biophysical Journal*. 108(2):407a.
- [7] Oelschlaeger C, Bossler F, Willenbacher N. Synthesis, Structural and Micromechanical Properties of 3D Hyaluronic Acid-Based Cryogel Scaffolds. *Biomacromolecules*. 2016;17(2):580-9.
- [8] Huang J, Wang L, Xiong C, Yuan F. Elastic hydrogel as a sensor for detection of mechanical stress generated by single cells grown in three-dimensional environment. *Biomaterials*. 2016;98:103-12.
- [9] Yuan B, Ritzoulis C, Chen J. Extensional and shear rheology of a food hydrocolloid. *Food Hydrocolloids*. 2018;74:296-306.
- [10] Papagiannopoulos A, Sotiropoulos K, Pispas S. Particle tracking microrheology of the power-law viscoelasticity of xanthan solutions. *Food Hydrocolloids*. 2016;61:201-10.

- [11] Mason TG, Weitz DA. Optical Measurements of Frequency-Dependent Linear Viscoelastic Moduli of Complex Fluids. *Physical Review Letters*. 1995;74(7):1250-3.
- [12] Papagiannopoulos A. Introduction to the most popular microrheology techniques. *Microrheology with Optical Tweezers: Principles and Applications*: Pan Stanford; 2016.
- [13] Crocker JC, Grier DG. Methods of Digital Video Microscopy for Colloidal Studies. *Journal of Colloid and Interface Science*. 1996;179(1):298-310.
- [14] Que R, Mohraz A, Da Silva NA, Wang S-W. Expanding Functionality of Recombinant Human Collagen Through Engineered Non-Native Cysteines. *Biomacromolecules*. 2014;15(10):3540-9.
- [15] Larsen TH, Furst EM. Microrheology of the Liquid-Solid Transition during Gelation. *Physical Review Letters*. 2008;100(14):146001.
- [16] Cingil HE, Rombouts WH, van der Gucht J, Cohen Stuart MA, Sprakel J. Equivalent Pathways in Melting and Gelation of Well-Defined Biopolymer Networks. *Biomacromolecules*. 2015;16(1):304-10.
- [17] Dong Y, Jin G, Ji C, He R, Lin M, Zhao X, et al. Non-invasive tracking of hydrogel degradation using upconversion nanoparticles. *Acta Biomaterialia*. 2017;55:410-9.
- [18] Ng SS, Su K, Li C, Chan-Park MB, Wang D-A, Chan V. Biomechanical study of the edge outgrowth phenomenon of encapsulated chondrocytic isogenous groups in the surface layer of hydrogel scaffolds for cartilage tissue engineering. *Acta Biomaterialia*. 2012;8(1):244-52.
- [19] Keating M, Kurup A, Alvarez-Elizondo M, Levine AJ, Botvinick E. Spatial distributions of pericellular stiffness in natural extracellular matrices are dependent on cell-mediated proteolysis and contractility. *Acta Biomaterialia*. 2017;57:304-12.
- [20] Braeckmans K, Buyens K, Bouquet W, Vervaet C, Joye P, Vos FD, et al. Sizing Nanomatter in Biological Fluids by Fluorescence Single Particle Tracking. *Nano Letters*. 2010;10(11):4435-42.
- [21] Naeye B, Deschout H, Röding M, Rudemo M, Delanghe J, Devreese K, et al. Hemocompatibility of siRNA loaded dextran nanogels. *Biomaterials*. 2011;32(34):9120-7.
- [22] Li W, Liu Q, Zhang P, Liu L. Zwitterionic nanogels crosslinked by fluorescent carbon dots for targeted drug delivery and simultaneous bioimaging. *Acta Biomaterialia*. 2016;40:254-62.
- [23] Jarzębski M, Bellich B, Białopiotrowicz T, Śliwa T, Kościński J, Cesàro A. Particle tracking analysis in food and hydrocolloids investigations. *Food Hydrocolloids*. 2017;68:90-101.
- [24] Moschakis T. Microrheology and particle tracking in food gels and emulsions. *Current Opinion in Colloid & Interface Science*. 2013;18(4):311-23.
- [25] Sotiropoulos K, Papagiannopoulos A. Modification of xanthan solution properties by the cationic surfactant DTMAB. *International Journal of Biological Macromolecules*. 2017;105:1213-9.
- [26] Moschakis T, Lazaridou A, Biliaderis CG. A micro- and macro-scale approach to probe the dynamics of sol-gel transition in cereal β -glucan solutions varying in molecular characteristics. *Food Hydrocolloids*. 2014;42:81-91.
- [27] Georgiades P, Pudney PDA, Thornton DJ, Waigh TA. Particle tracking microrheology of purified gastrointestinal mucins. *Biopolymers*. 2014;101(4):366-77.
- [28] Henry CE, Wang Y-Y, Yang Q, Hoang T, Chattopadhyay S, Hoen T, et al. Anti-PEG antibodies alter the mobility and biodistribution of densely PEGylated nanoparticles in mucus. *Acta Biomaterialia*. 2016;43:61-70.
- [29] Lai SK, Suk JS, Pace A, Wang Y-Y, Yang M, Mert O, et al. Drug carrier nanoparticles that penetrate human chronic rhinosinusitis mucus. *Biomaterials*. 2011;32(26):6285-90.
- [30] Brancato V, Garziano A, Gioiella F, Urciuolo F, Imparato G, Panzetta V, et al. 3D is not enough: Building up a cell instructive microenvironment for tumoral stroma microtissues. *Acta Biomaterialia*. 2017;47:1-13.
- [31] Francis AC, Melikyan GB. Live-Cell Imaging of Early Steps of Single HIV-1 Infection. *Viruses*. 2018;10(5):275.
- [32] Francis AC, Marin M, Shi J, Aiken C, Melikyan GB. Time-Resolved Imaging of Single HIV-1 Uncoating In Vitro and in Living Cells. *PLoS Pathogens*. 2016;12(6):e1005709.